

COMPOSITION AND PARTICLE-SIZE EVOLUTION OF KENTUCKY #9

Thomas Erickson, Christopher Zygarlicke, Murali Ramanathan, and Bruce Folkedahl
University of North Dakota Energy and Environmental Research Center
Box 8213, University Station
Grand Forks, ND 58202

Keywords: coal, inorganic transformations, predictive method

INTRODUCTION

The size and composition of ash resulting during coal combustion involves both chemical and physical processes. Ash particles formed during coal combustion depend largely upon the association of the inorganic species in the coal. In order to accurately model the ash formation processes, detailed information on the distribution of minerals with respect to coal particles is essential.

The combustion of Kentucky #9 coal was analyzed through a three-step approach to track particle-size and compositional evolution. First, the coal was characterized with advanced analytical techniques to determine the original size and type of the minerals present. Second, the coal was combusted under carefully controlled conditions to produce fly ash. The fly ash was characterized with analytical techniques similar to those used with the coal. Third, two separate predictive methods were produced from comparison of the two data sets as well as previous investigations (1,2).

EXPERIMENTAL APPROACH

A utility-sized (70% -200 mesh) sample of Kentucky #9 coal was received from the coal sample bank at Foster Wheeler. The coal was characterized by computer-controlled scanning electron microscopy (CCSEM), x-ray fluorescence (XRF), proximate-ultimate analysis, and automated- and manual-imaging techniques in conjunction with the CCSEM technique. The above analysis combined to provide a wide base of knowledge on the coal in terms of the minerals present, their size distributions, and the bulk chemistry of the coal.

The coal was combusted in a vertically oriented laminar flow furnace (drop-tube furnace) at 1500°C, for approximately 2.5 seconds in an environment to simulate the fouling conditions present during combustion in a pulverized coal-fired furnace. The ash was immediately cooled and quenched with nitrogen upon leaving the furnace. The resultant ash was analyzed with CCSEM. The information obtained from the ash is particle size and particle composition.

COAL AND ASH CHARACTERIZATION

The CCSEM data for both the coal and the formed fly ash were analyzed with the use of a classification method, designed by UNDEERC, specifically for CCSEM data. The fly ash data was first corrected for the spherical orientation of the particles. Figure 1 is a SEM photograph of the fly ash produced and shows that a spherical (circular) orientation of the particles is predominant. When analyzing the size of spheres with a random, cross-sectional, two-dimensional technique, the average measured diameter is lower than the actual average diameter (3). The following equation was applied to correct for this underestimation:

$$D_A = D_M * 4/\pi \quad [\text{Eq. 1}]$$

where D_A is the actual diameter and D_M is the measured diameter. Table 1 shows the compositional classifications as determined from the CCSEM analysis for both the coal and fly ash. It is noted that the classification of CCSEM data is not specific to crystalline types; it classifies by composition only. Figure 2 shows the

particle-size distribution for the coal and fly ash (corrected for spherical orientation) as determined by CCSEM. The reason for the fly ash distribution being smaller than the mineral size distribution can only be from the fragmentation of mineral particles during combustion. Since pyrite is the only major mineral classified to undergo fragmentation under combustion conditions, and it comprises a substantial amount of the minerals, an "iron-free basis" may give a better understanding of the transformations that occur. Figure 3 shows both the mineral and fly ash distributions on an "iron-free basis." The mineral distribution is now smaller than the fly ash which shows evidence of coalescence of minerals during combustion. Table 2 shows the new classification of the two samples on an "iron-free basis."

The coal was also investigated for the inclusion of minerals inside coal particles (inherent) and the presence of minerals not associated inside a carbon structure (extraneous) (4). Figure 4 shows an SEM photograph of a cross section of the coal mounted in epoxy. The minerals (brighter areas) can be seen to exist in both the coal (grey areas) and epoxy (dark areas). Every particle classified with the CCSEM routine (>2000 particles) was also classified as inherent or extraneous.

PREDICTIVE METHOD 1

Method 1 uses the coal CCSEM results on an "iron-free basis" to predict fly ash formation on an "iron-free basis." The iron-containing species are omitted with the assumption that they lead primarily to the formation of iron oxide and small amounts of iron rich aluminosilicates and silicates. The two categories used in Method 1 are inherent and extraneous particles. The extraneous particles are assumed to not interact with other extraneous or inherent particles during the combustion process. The inherent particles are assumed to randomly coalesce during the process. A random number (with upper and lower limits) of the inherent particles is chosen at random and coalesced to form a single fly ash particle. The sizes and compositions of the coalescing particles are used to generate the size and composition of the resulting fly ash particles. 3000 particles are created from the inherent data and processed through the CCSEM classification program. The inherent and extraneous compositions are combined to form the resultant data. Table 3 shows the composition of the particles produced by Method 1, along with the experimental fly ash composition. Both compositions are similar with differences noted with aluminosilicate particles. A likely explanation for the difference is that the CCSEM classification program incorporates a large number of aluminosilicate classifications and thus must draw fine lines from classification to classification. The total aluminosilicates found for Method 1 and experimental ash are 54.8 and 55.3, respectively, which supports the above statement. The particle-size distributions for both the experimental data and predictive Method 1 are shown in Figure 5. The distributions are very close, and a slight modification in coalescence extremes would be expected to fit better with little change in composition.

PREDICTIVE METHOD 2

Method 2 does not involve the "iron-free basis" of the previous method. The entire data set is used, and predictions are on a total basis. The role in inherent and extraneous particles are similar to Method 1. The inherent pyrite is allowed to coalesce with a small loss in volume due to the release of sulfur during combustion. The extraneous pyrite is assumed to produce iron oxide in a reduced amount also due to the release of sodium. Table 4 shows the compositions predicted, along with those of the fly ash. The iron oxide composition appears to be very high and is believed to be a result of sampling error prior to CCSEM analysis. The pyrite analyzed here is almost double that of a previous reporting. By reducing the pyrite (\rightarrow iron oxide) and renormalizing the data, a much closer composition is achieved and is also shown in Table 4.

CONCLUSIONS

Method 1 shows very good agreement with the experimental fly ash data. The use of an iron-free basis allows the study of direct coalescence of minerals in the absence of mineral fragmentation. A proper algorithm for iron removal is essential, and previous results used assumptions that may induce limited amounts of error.

Method 2, with the correction in pyrite to fit previously reported values, also looks very good. At the current time, the investigation of pyrite fragmentation is crucial in determining the total size distribution of the ash; thus it has not been addressed here.

CCSEM analysis coupled together with inherent and extraneous classifications are showing great promise for predicting fly ash formation from coal data. The next step is a coal particle-by-coal particle analysis technique.

REFERENCES

1. Zygarlicke, C.J.; Toman, D.L.; Benson, S.A. "Trends in the Evolution of Fly Ash Size During Combustion," Prepr. Pap.--Am. Chem. Soc., Div. Fuel Chem. 1990, 35(3), 621-636.
2. Zygarlicke, C.J.; Steadman, E.N.; Benson, S.A. "Studies of Transformation of Inorganic Constituents in a Texas Legnite during Combustion," Progress in Energy and Combustion. Science Review, 1990, 16, 195-204.
3. Zygarlicke, C.J.; Toman, D.L.; Steadman, E.N.; Brekke, D.W.; Erickson, T.A. "Combustion Inorganic Transformation," Quarterly Technical Progress Report to United States Department of Energy on Contract No. DE-FC21-86MC10637; University of North Dakota Energy and Environmental Research Center, Grand Forks, ND, 1990.
4. Zygarlicke, C.J.; Steadman, E.N. "Advanced SEM Techniques to Characterize Coal Minerals," Scanning Microscopy 1990, 4(3), 579-590.

TABLE 1

CCSEM RESULTS FOR THE MAJOR COMPONENTS OF KENTUCKY #9 COAL AND FLY ASH

<u>Classifications</u>	<u>Coal</u>	<u>Fouling Ash</u>
Quartz	9.5	8.4
Iron Oxide	0.2	11.2
Calcite	1.0	2.2
Kaolinite	4.3	2.5
Montmorillonite	3.8	6.3
K-Aluminosilicate	13.6	15.2
Fe-Aluminosilicate	0.1	9.9
Aluminosilicate	0.5	6.7
Mixed Aluminosilicate	0.2	5.0
Pyrite	44.7	1.5
Si-Rich	2.4	8.7
Unknowns	16.2	17.5

TABLE 2

IRON-FREE MAJOR COMPONENTS OF KENTUCKY #9 COAL AND FLY ASH

<u>Classifications</u>	<u>Coal</u>	<u>Fouling Ash</u>
Quartz	17.70	10.9
Calcite	3.00	2.9
Kaolinite	8.00	6.0
Montmorillonite	10.50	14.4
K-Aluminosilicate	36.00	22.5
Aluminosilicate	2.45	10.7
Mixed Aluminosilicate	0.70	1.7
Si-Rich	6.20	11.9
Unknowns	8.30	9.7

TABLE 3

COMPARISON OF PREDICTIVE METHOD 1 AND EXPERIMENTAL FLY ASH DATA
ON AN IRON-FREE BASIS

<u>Classifications</u>	<u>Method 1</u>	<u>Fouling Ash</u>
Quartz	12.9	10.9
Calcite	2.7	2.9
Kaolinite	5.6	6.0
Montmorillonite	10.8	14.4
K-Aluminosilicate	33.9	22.5
Aluminosilicate	4.0	10.7
Mixed Aluminosilicate	0.5	1.7
Gypsum	2.3	1.9
Apatite	2.6	0.5
Si-Rich	8.2	11.9
Unknown	12.8	9.7

TABLE 4

COMPARISON OF PREDICTIVE METHOD 2 AND EXPERIMENTAL FLY ASH COMPOSITION
 (A modification of Method 2 is also shown due to the inconsistency of pyrite.)

Classifications	Method 2	Fouling Ash	Modified
Quartz	8.0	8.4	9.3
Iron Oxide	30.0	11.2	15.6
Calcite	1.6	2.2	1.9
Kaolinite	2.6	2.5	3.0
Montmorillonite	4.4	6.3	5.1
K-Aluminosilicate	19.3	15.2	22.5
Fe-Aluminosilicate	4.7	9.9	5.4
Aluminosilicate	2.1	6.7	2.4
Mixed Aluminosilicate	0.4	5.0	0.4
Gypsum	1.4	1.5	1.6
Apatite	1.6	0.4	1.9
Si-Rich	4.7	8.7	5.5
Unknowns	17.7	17.5	19.9

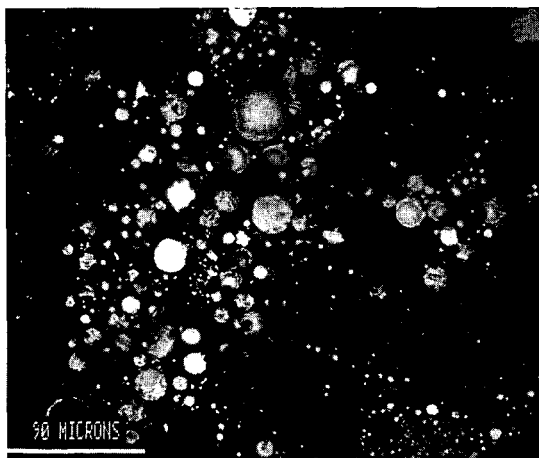


Figure 1. SEM photograph of Kentucky #9 fly ash formed under fouling conditions at 1500°C for 2.5 seconds.

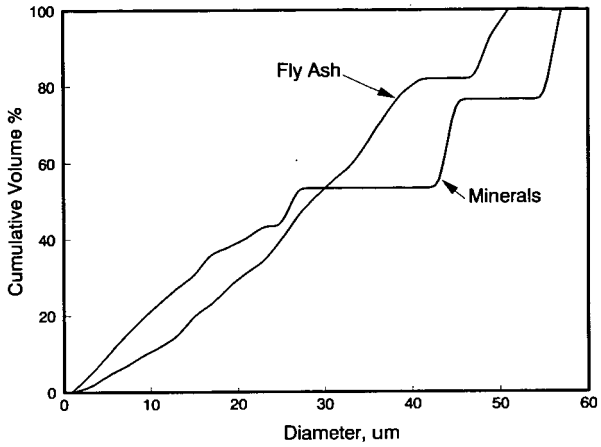


Figure 2. CCSEM particle-size distributions for Kentucky #9 coal and fly ash.

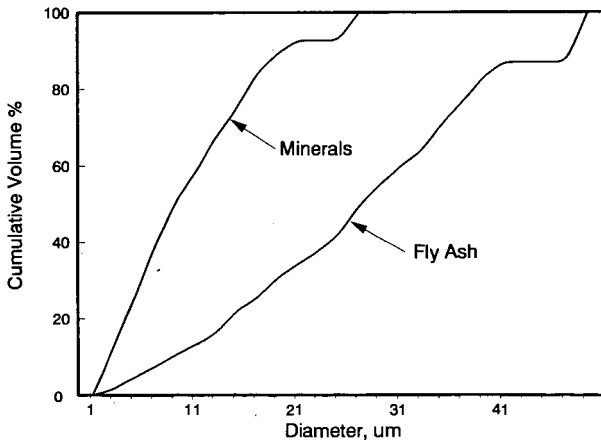


Figure 3. Iron-free particle-size distribution for Kentucky #9 coal and fly ash.

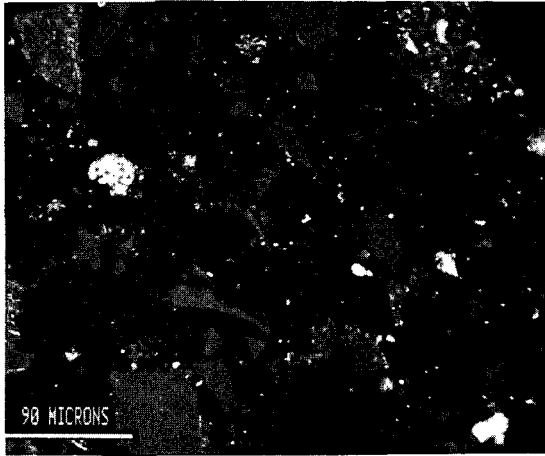


Figure 4. SEM (BEI) photograph of Kentucky #9 coal mounted in epoxy. Bright area - minerals, grey area - coal, dark area - epoxy.

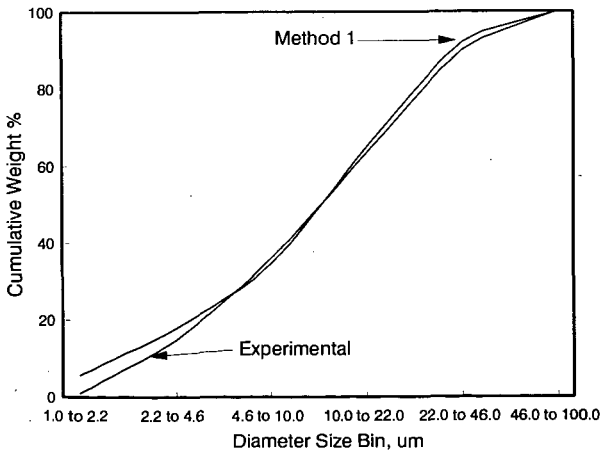


Figure 5. Particle-size distributions of experimental fly ash and predictive Method 1 particles on an iron-free basis.